Solar energy dissipation and temperature control by water and plants

Jan Pokorný*

ENKI, o.p.s.,
Dukelská 145, CZ-379 01 Třeboň, Czech Republic
E-mail: pokorny@enki.cz
*Corresponding author

Jakub Brom

Faculty of Agriculture,
Department of Landscape Management,
University of South Bohemia,
Studentská 13, CZ-370 05 České Budějovice, Czech Republic

and

ENKI, o.p.s.,
Dukelská 145, CZ-379 01 Třeboň, Czech Republic
E-mail: jbrom@zf.jcu.cz

Jan Čermák

Faculty of Forestry and Wood Technology,
Institute of Forest Botany,
Dendrology and Geobiocenology,
Mendel University in Brno,
Zemědělská 3, CZ-61300 Brno, Czech Republic
E-mail: cermak@mendelu.cz

Petra Hesslerová

ENKI, o.p.s.,
Dukelská 145, CZ-379 01 Třeboň, Czech Republic

and

Faculty of Environmental Sciences,
Dept. of Applied Geoinformatics and Spatial Planning,
Czech University of Life Sciences Prague,
Kamýcká 129, Praha 6 – Suchdol, CZ-165 21, Czech Republic
E-mail: hesslerova@enki.cz

Hanna Huryna

Institute of Physical Biology,
University of South Bohemia,
CZ-373 33 Nové Hrady, Czech Republic
E-mail: hanna.huryna@gmail.com

Nadia Nadezhdina

Faculty of Forestry and Wood Technology,
Institute of Forest Botany,
Dendrology and Geobiocenology,
Mendel University of in Brno,
Zemědělská 3, CZ-61300 Brno, Czech Republic
E-mail: nadezdan@mendelu.cz

Alžběta Rejšková

ENKI, o.p.s.,
Dukelská 145, CZ-379 01 Třeboň, Czech Republic
E-mail: betuse@seznam.cz

Abstract: Ecosystems use solar energy for self-organisation and cool themselves by exporting entropy to the atmosphere as heat. These energy transformations are achieved through evapotranspiration, with plants as 'heat valves'. In this study, the dissipative process is demonstrated at sites in the Czech Republic and Belgium, using landscape temperature data from thermovision and satellite images. While global warming is commonly attributed to atmospheric CO_2, the research shows water vapour has a concentration two orders of magnitude higher than other greenhouse gases. It is critical that landscape management protects the hydrological cycle with its capacity for dissipation of incoming solar energy.

Keywords: ecosystems; evapotranspiration; sensible heat; albedo; radiative forcing; temperature variation; remote sensing.

Reference to this paper should be made as follows: Pokorný, J., Brom, J., Čermák, J., Hesslerová, P., Huryna, H., Nadezhdina, N. and Rejšková, A. (2010) 'Solar energy dissipation and temperature control by water and plants', *Int. J. Water*, Vol. 5, No. 4, pp.311–336.

Biographical notes: Jan Pokorný took his PhD at the Charles University, worked on photosynthetic processes at the Agricultural University, Prague, and later headed the Třeboň Section of the Institute of Botany at the Czech Academy of Sciences. Among his many commitments, he directs ENKI, a public benefit corporation for environmental research. Outside Europe, he has worked in Africa and Australia, and in 1998 was elected to the Scientific Technology Review Panel of the Ramsar Convention. His 200 publications include *Macrophyte Photosynthesis and Aquatic Environment*, Rozpravy of Czechoslovak Academy of Sciences. Academia: Praha (1991).

Jakub Brom is a researcher in the Faculty of Agriculture at the University of South Bohemia in České Budějovice, Czech Republic; he also contributes to

the public benefit corporation ENKI in Třeboň. His interests are the physiological ecology of plants and bioclimatology, mostly researched using meteorological methods, thermometry and remote sensing. He is the co-author of several papers in peer-reviewed journals, including 'Temperature and humidity characteristics of two willow stands, a peaty meadow and a drained pasture and their impact on landscape functioning' (*Boreal Env. Res.*, 2009).

Jan Čermák studied forestry at the Mendel University of Brno Czech Republic and received his PhD from the same university. He has over 30 years of teaching experience in whole tree water relations, architecture and growth. He has performed collaborative research throughout Europe, Harvard, Washington University and the US Forest Service. He has served as Vice-Chair of the Whole Tree Physiology IUFRO association and on the editorial review board of *Tree Physiology*. His 270 published papers and 60 reports are widely cited (see: 'Application of sap flow technique for characterising the whole tree architecture, especially root distribution', *Acta Horticulturae*, 2009).

Petra Hesslerová graduated in Physical Geography and Geoecology at the Charles University, Prague, where she also received her PhD in 2008. She currently works for the ENKI public benefit corporation and is an Assistant Lecturer at the Czech University of Life Sciences, Prague. Her specialisations are geography, remote sensing and landscape ecology, carried out in cross-national contexts. She has co-authored a number of publications including: 'The synergy of solar radiation, plant biomass, and humidity as an indicator of ecological functions of the landscape', *Integr. Env. Assessm. Managem.* (2010).

Hanna Huryna graduated in Natural Resources and Ecology at the Belorussian National Technical University, Minsk. She later worked with the Belarusian Scientific Institute for Transport Research. She is currently a PhD student in the Institute for Physical Biology at the University of South Bohemia, Nove Hrady, Czech Republic. Her publications include: 'Comparison of reflected solar radiation, air temperature and relative air humidity in different ecosystems' in Vymazal, J. (Ed.): *Water and Nutrient Management in Natural and Constructed Wetlands* (forthcoming 2010).

Nadia Nadezhdina studied in Archangelsk and Gorky, Russia, and has a PhD from the Ukrainian Academy of Sciences, Kiev. She is currently Professor in the Institute for Forest Botany at the Mendel University, Brno, Czech Republic. She has joined many international research collaborations including Europe, China and the USA. She holds 11 patents on physiological equipment and has 120 papers and 20 research reports on eco-physiology and innovative methods for the study of tree water relations and architecture (see: 'Integration of water transport pathways in a maple tree: responses of sap flow to branch severing', *Ann. For. Sci.*, 2010).

Alžběta Rejšková took her MA at the Charles University in Prague, and in 2009 completed a PhD at the University of South Bohemia. Her main research interest is the eco-physiology of plants and the role of vegetation in landscape functioning. She currently works for the public benefit corporation ENKI and is an external lecturer in the Department of Plant Physiology at the Charles University. She has co-authored 'Temperature distribution in light-coloured flowers and inflorescences of early spring temperate species measured by infrared camera', *Flora* (2010).

1 Introduction

This paper demonstrates the fundamental role played by water and vegetation in maintaining local climate. Human modification of a landscape by deforestation, industrial agriculture and urbanisation may destroy the capacity of an ecosystem to dissipate – digest and distribute – solar energy fluxes. On a hard dry surface, sensible heat can be released to several hundred watts/m^2, but water or vegetated surfaces have the capacity to convert solar energy into the latent heat flux of vaporisation. Evaporation allows latent heat, in the form of water vapour, to be carried to cooler places where it condenses and releases heat. The amount of energy and heat moved in this way should not be underestimated. On a sunny day, a flux of solar energy falling on 2 km^2 of ground may be equivalent to the power generated by a large nuclear power station (2000 MW). Ultimately, it becomes a matter of public education and political choice as to how these natural processes are treated. Either the solar flux is permitted to provide the natural air-conditioning of water vaporisation and plant growth or it is converted into sensible heat and environmental temperatures soar to 40–50°C.

1.1 Solar energy flux between Sun and Earth

It is the Sun's energy that drives the water cycle, plant production and other processes, which cause equilibrium shifts in the biosphere and which enable its development. Solar energy warms the Earth to an average temperature of around 15°C or 288 K. For a mean distance between the Sun and the Earth, the intensity of solar radiation incident upon a surface perpendicular to the Sun's rays measured above the atmosphere is approximately 1367 W m^{-2}. This quantity is called the solar constant. The solar constant is very stable, fluctuating ±1.3 W m^{-2} (0.1%) during the 11-year period of sun spot cycles. The actual direct solar irradiance at the top of the Earth's atmosphere fluctuates during a year from 1412 W m^{-2} in early January to 1321 W m^{-2} in early July due to the Earth's varying distance from the Sun. The amount of solar energy changes over the year by about ±3.2% (45 W m^{-2}) depending on the position of Earth in its elliptic orbit around the Sun (Geiger et al., 2003; Kopp et al., 2005). The Sun as a blackbody with a surface temperature of 5900 K emits a maximum radiation in the visible range of 400–700 nm. The surface of the Earth with its temperature ca. 288 K emits a maximum radiation in the infrared (IR) part of the spectrum of about 10 μm. The atmosphere influences the spectrum of incident light both quantitatively and qualitatively. The spectrum of solar radiation incident on both the Earth's atmosphere and the surface at sea level is shown in Figure 1 where the absorption of radiation through the main atmospheric gases is indicated.

The amount of received solar energy varies across the world and varies in daily and seasonal pulses. The mean distributions of global insulation for different months are to be found in the pages of NASA SSE (http://eosweb.larc.nasa.gov/sse). According to NASA SSE data, the maximum annual average direct normal radiation incident on the Earth's surface is up to 10 GJ m^{-2} (2770 kWh m^{-2}), with maximum monthly average direct normal radiation 30 MJ m^{-2} day^{-1} (8.5 kWh m^{-2} day^{-1}). This intensity of solar radiation is reached, for example, along the northwest coast of Australia. In the Czech Republic, which is a temperate zone, the annual income of solar radiation is about 4.14 GJ m^{-2} (1150 kWh m^{-2}); in Helsinki (Finland) 3.49 GJ m^{-2} (970 kWh m^{-2}) and in Giza (Egypt) 7.45 GJ m^{-2} (2070 kWh m^{-2}).

The maximum irradiance commonly lies between 800 W m^{-2} and 1000 W m^{-2} in the tropics and subtropics and during the growing season in temperate zones. This indicates that approximately 25–40% of energy incident on the upper layer of the atmosphere is reflected, scattered or absorbed in the atmosphere and does not reach the Earth's surface. The transmission of solar radiation is a function of two variables:

- path length through the atmosphere across which the solar beam travels
- the content of absorbers present in the atmosphere.

Figure 1 Solar spectrum incident on the atmosphere and on the Earth's surface at sea level. Radiation of the blackbody of 5900 K is also shown. Seven gases in the Earth's atmosphere produce observable absorption features in the 0.4–2.5 mm range: water vapour, carbon dioxide, ozone, nitrous oxide, carbon monoxide, methane and oxygen. (http://www.csr.utexas.edu/projects/rs/hrs/process.html). 1 Å = m^{-10}

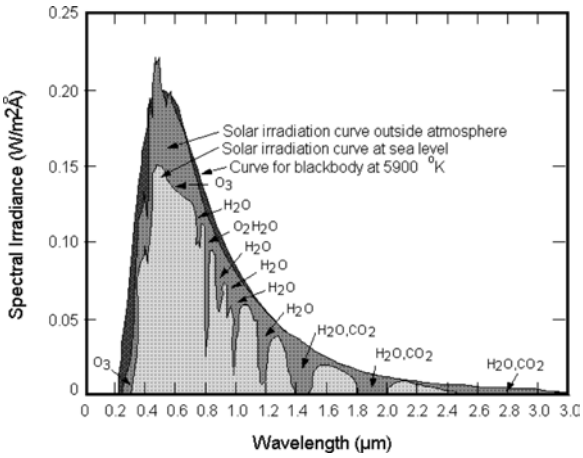

By far, the most variable and dynamic absorber is water vapour. The amount of incoming energy differs significantly also with weather conditions. The difference between the amounts of incoming radiation on a clear day (e.g., 29.3 MJ m^{-2} and maximum flux 1000 W m^{-2}) can be an order of magnitude higher than the amount of incoming radiation on an overcast day (e.g., 0.78 kWh m^{-2}, maximum flux 100 W m^{-2}). The distribution of solar energy on the Earth depends on its surface characteristics. Part of the energy is reflected straight away after incidence. The ratio of reflected to incident radiation is called albedo. Dark surfaces such as water, wet soil and wet vegetation absorb solar radiation whereas light surfaces like snow or sand are more reflective. The sum of all incoming radiation minus all outgoing radiation across a unit area of the plane is called net radiation (R_n). The IR part of radiation contributes to radiation balance – the sky is commonly colder than the Earth's surface, which results in energy loss from the Earth's surface.

1.2 Distribution of solar energy in ecosystems

There is a big difference between the distribution of net radiation in functioning natural ecosystems of high plant biomass well supplied with water vs. dry non-living physical surfaces. In ecosystems, net radiation (R_n) is divided in varying proportion into the

following four parts: latent heat flux (LE), sensible heat flux (H), ground heat flux (G) and storage of energy (S). It can be described using the following equation:

$$R_n = \mathrm{LE} + \mathrm{H} + \mathrm{G} + \mathrm{S}. \quad (1)$$

The latent heat flux (LE) represents the energy used for evaporation of water from the surface. The transition of liquid into a gas phase is an endothermic reaction, i.e., energy consumption, and thus local cooling accompanies it. On the contrary, condensation is an exothermic process attended by energy release and local warming. An amount of 2.45 MJ (0.68 kWh) of energy is needed for the evaporation of 1 kg water at 20°C; the same amount of energy is released during condensation of 1 kg water vapour. The dynamic system of phase transitions of water plays a crucial role in thermoregulation of living systems and in damping temperature differences on the Earth.

Plants transport water with nutrients from soil via their roots and stems into leaves from where water evaporates – a process called transpiration. The evaporation of water from plant stands is called evapotranspiration, as it consists of transpiration and evaporation both from soil and from intercepted water from the plant's surface. The rate of ET from stands of vegetation supplied with water reaches several litres of water per day per square metre. ET of 4 kg m^{-2} day^{-1} represents mean daily flux of latent heat 225 W m^{-2} (calculated for 12 daylight hours). The horizontal movement of energy, called advection, amplifies ET substantially. Advection is horizontal convective heat transport both of sensible and of latent heat (Oke, 1987) and it can have significant effects on energy exchange and on a vegetation-water regime (see e.g., Li and Yu, 2007). A hot, dry wind blowing on to a moist oasis evaporates more water than can be calculated by the vertical accounting of energy budgets (Monteith, 1975). Because of the effect of advection, ET values can exceed 15 mm per day (Kučerová et al., 2001).

The sensible heat flux (H) represents the sum of all heat exchanges between the surface of a landscape and its surroundings by conduction or convection. It is positive when the surface is warmer than surroundings and heat is lost from it. The sensible heat flux is negative when heat moves in the opposite way. The proportion of sensible heat in the energy balance of an ecosystem increases when water is not present, since the capacity for evaporative cooling by latent heat is diminished. On dry surfaces, the sensible heat flux may reach values of several hundreds of Wm^{-2}. The sensible heat of an overheated surface warms air, which rises up in a turbulent motion creating atmospheric instability.

The ground heat flux (G) is positive when the ground is warming. G is commonly positive during the day and negative at night. The heat balance of the ground is usually moderately positive during warm periods and negative during the cold periods, making the net yearly ground heat-flux approach zero. During the plant growing period in daylight hours, G ranges from 2% of R_n in a dense vegetation canopy to more than 30% of R_n in sparse canopies with little shading of the soil (Jones, 1992). A layer of organic matter like dry leaves and bark will insulate soil from energy coming in from its surroundings. The heat conductivity of soil increases with its water content (Peters-Lidard et al., 1998). The energy stored in vegetation is the smallest part of R_n. Principally, there are two energy sinks within a plant stand

- metabolic sink, i.e., photosynthesis with consequent biomass production
- a physical sink, which represents heating of the plant material itself.

In closed canopy ecosystems, the maximum net photosynthesis rate is 1.0–1.4 mg m^{-2} s^{-1} of sucrose (Cooper, 1975), which corresponds to 17.0–23.4 J of energy fixed every second, i.e., energy flux 17.0–23.4 W m^{-2}. This represents about 2% of total summer irradiance and about 3% of R_n, on the assumption that it should be approximately 700 W m^{-2}. The physical sink of energy depends on the amount of living biomass, which contains about 90% of water. Assuming that 2.2 kg m^{-2} of fresh biomass containing approximately 2 kg of water was warmed up to 4°C per hour, then the heat-flux warming the biomass would be approximately 10 W m^{-2} (heat capacity of water is 4184 J kg^{-1} K^{-1} at 20°C). Contrary to biomass production, the decomposition of organic matter is associated with release of energy. The rate of decomposition can be several times higher than the rate of biomass production, i.e., release of heat due to decomposition can reach several tens of W m^{-2}. The decomposition of organic matter in soil is accelerated by drainage.

1.3 Exchange of water and CO_2 in plant stands

Most plant tissues contain large amounts of water. The biomass of non-woody tissues typically comprises 80–95% of water. Most water taken up by roots is transported through plants in the Soil-Plant-Atmosphere Continuum (SPAC) and transpired into the air. Transpiration is vital to the uptake of CO_2 in the intercellular air spaces of stomata (Berry et al., 2005). The cooling process of transpiration is often considered a side effect rather than a mechanism to control leaf temperature (Lambers et al., 1998). Transpiration is also perceived as a rather negative process. Plant physiology and hydrology may use negative terms such as 'transpiration loss' and 'evapotranspiration losses'. Transpiration Efficiency (TE) is defined as the amount of water lost through transpiration per unit of dry matter produced. TE normally reaches a value of several hundred kilograms of water consumed per kilogram of dry biomass produced. The amount of water molecules exchanged by plants is at least two orders of magnitude higher than the amount of carbon dioxide fixed to biomass (You et al., 2009).

The average concentration of CO_2 in the air is about 391 ppm (NOAA, 2010). In plant stands, the concentration of CO_2 varies both by vertical profile measures and by day and night, depending on the photosynthetic and respiration activities of biota. On the leaf surface of C4 plants such as corn, the concentration of CO_2 falls to zero whereas on a forest floor, CO_2 concentration can be over 500 ppm (Jassal et al., 2007). Conventional climate models, as well as calculations of the global carbon budget, treat the concentration of CO_2 in the atmosphere as homogeneous (Randerson et al., 2006).

In contrast to CO_2 as a greenhouse gas, the amount of water vapour as a greenhouse gas found in plant stands and in the atmosphere is many times higher and it changes dramatically across time and space. For example, air saturated with water at 21°C contains 18 g m^{-3} of water vapour, i.e., 22,400 ppm. Air saturated with water at 40°C contains 50 g m^{-3} of water vapour, i.e., 62,200 ppm. The amount of water vapour in air is often two orders of magnitude higher than that of CO_2. Water absorbs solar energy in visible, near and far IR. The energy absorption spectrum of water is broader than that of CO_2 (see Figure 1). The content of water vapour in the atmosphere is highly variable, and furthermore, water exists in three phases (solid, liquid and gaseous). The transitions between these phases are linked with the uptake or release of high amounts of energy. Climate change and global warming are reputedly caused by an increase in CO_2

concentration from 250 ppm to 390 ppm. The present research highlights the dynamic role of water vapour, with its concentration two orders of magnitude higher than that of other greenhouse gases. The implication is that human landscape management affects the behaviour of water vapour and its role in the dissipation of solar energy.

2 Site description and methods

Seven different sites were monitored in this study: five non-forested and two forested areas. Non-forested areas were located in the Třeboň Biosphere Reserve, Czech Republic; the forested areas were in South Moravia, Czech Republic and in Antwerp province, Belgium.

Exact methods for the monitoring and evaluation of energy fluxes were used to assess:

- seasonal series of incoming and reflected solar radiation, albedo and temperature
- daily series of main fluxes of solar energy (incoming and reflected solar energy, sensible, latent and ground heat fluxes)
- temperature distribution in landscape monitored by remote sensing
- transpiration of trees measured by sap flow method and expressed in terms of energy transition.

2.1 Třeboň Basin Biosphere Reserve (TBBR)

This research area is situated in the southern part of Bohemia at the Austrian–Czech border. The basin is mostly filled with sand and clay sediments while the marginal parts consist of igneous crystalline rocks. The flat bottom of the basin is 410–470 m altitude; the undulating marginal area reaches 550 m. The Třeboň Basin belongs to a moderately warm region with an annual mean temperature of 8°C and a mean annual precipitation total of 650 mm. Forest covers about 50% of the territory. The Basin is marked by a sophisticated network of human-made canals and watercourses built since the Middle Ages for drainage of wetlands and the construction of fish ponds. The TBBR with a total area of 700 km^2 has about 500 fish ponds making a total area 7500 ha. Forestry, agriculture and fishing are main activities in TBBR (Jeník and Květ, 2002). The study sites are several km apart.

Data were collected at the following sites:

- Autumn barley field (area of 22 ha).
- Wet Meadow (area of c. 200 ha) in the Rožmberk fish pond (450 ha) floodplain. Dominant macrophyte species include high sedges (*Carex gracilis* (L.), *Carex vesicaria* (L.)), *Calamagrostis canescens* (Weber), *Phalaris arundinacea* (L.) and *Urtica dioica* (L.) The area surrounding the meteorological station is not managed; tall vegetation is cut only close to the station. The dryer parts of the Wet Meadow are mowed once a year.
- Concrete surface (area of 400 m^2) within the area of the Wastewater Treatment Plant of the city of Třeboň.

- Open water surface of the Ruda fish pond (72 ha, depth c. 2 m).
- Meadow is represented mostly by mesic vascular plant species: *Alopecurus pratensis* (L.), *Arrhenatherum elatius* (*L.*), *Phleum pratense* (L.), *Tanacetum vulgare* (L.) and *Taraxacum sect. Ruderalia*. This locality is mulched two or three times per year.

2.1.1 Forested sites in Moravia and Belgium

The first forested site is near Lednice in the southern part of Moravia in the alluvium of the Dyje River and classified as *Ulmeto-fraxinetum carpineum*. The soils of this locality originate from sedimentation during spring floods. The stand is composed mostly of oak (*Quercus robur* (L.) 78%, *Fraxinus excelsior* (L.) 18%, *Tilia cordata Mill*. 3% and 1% of other species) with the mean age of dominant trees 95 years and stand density of 90%. The leaf area index is 5 for the tree layer and 2 for the shrub layer (Vasicek, 1985; Čermák, 1998).

The second experimental plot of Scots pine (*Pinus sylvestris* (L.)) is a forest plantation in Brasschaat, Campine region of the province of Antwerp, Belgium, in a plateau of the northern lower plain basin of the Scheldt River. The original climax vegetation in the area is a *Querceto-Betuletum*. Soil is characterised as moderately wet and sandy with a distinct humus or iron B-horizon (psammenti haplumbrept in the USDA classification, umbric regosol or haplic podzol in the FAO classification). The experimental pine stand was 66-years old at the time of study. The original, homogeneous stocking density was relatively high for pine and the stand had been frequently thinned, most recently in 1993. Leaf area index (one side) was 3 (Čermák et al., 1998).

2.2 Meteorological data and energy balance

All measurements were made in the Třeboň Biosphere Reserve except measurements of tree transpiration. Meteorological data were recorded at 10-minute intervals during the growing season, 1 April–30 September 2008. Air temperature was measured 2 m above the soil surface and at the vegetation surface (T_a and T_c, °C; T+Rh probes, accuracy ±0.1°C). Temperature at the soil surface was measured by Pt 100 thermometer (T_s, °C; accuracy ±0.1°C). Incoming ($R_{s\downarrow}$) and reflected shortwave (global) radiation ($R_{s\uparrow}$) was measured on each site by CM3 pyranometers (Kipp & Zonen, the Netherlands, spectral range from 310 nm to 2800 nm). Incoming and emitted long-wave radiation was measured on the Meadow site by a CNR1 Net radiometer (Kipp & Zonen, the Netherlands, spectral range from 5 μm to 50 μm). The volumetric content of liquid water in the soil at 0.05 m below the surface was measured by (θ, %; Wirrib, AMET, Czech Republic, accuracy ±0.01 $m^3\ m^{-3}$). Emitted long-wave radiation ($R_L\uparrow$, $W\ m^{-2}$) was computed using Stefan-Boltzmann's law from temperature measured at the vegetation surface. Sky temperature calculated from net radiometer data was as follows (Monteith and Unsworth, 1990):

$$R_{L\uparrow} = \varepsilon\sigma T^4 \tag{2}$$

where ε is the emissivity of the surface (tabulated values were used according to Gates (1980)), σ is Stefan-Boltzman constant ($5.6703 \times 10^{-8}\ W\ m^{-2}\ K^{-4}$) and T is temperature (K).

Albedo (α, rel.) was computed as a ratio between reflected and incoming short-wave radiation:

$$\alpha = \frac{R_{S\uparrow}}{R_{S\downarrow}}. \tag{3}$$

Net radiation was computed from the short- and long-wave parts of radiation using equation (Brutsaert, 1982):

$$R_N = R_{S\downarrow} - R_{S\uparrow} + R_{L\downarrow} - R_{L\uparrow}. \tag{4}$$

Ground heat flux was computed using the vertical profile method described in Monteith and Unsworth (1990).

$$G = k\frac{\Delta T}{\Delta z} \tag{5}$$

where k is the soil thermal conductivity (W m^{-1} K^{-1}), ΔT is the temperature profile in the soil and Δz is the depth of this profile (m).

Latent and sensible heat fluxes were computed using the Bowen ratio method (Brutsaert, 1982; Monteith and Unsworth, 1990):

$$LE = \frac{R_N - G}{1+\beta} \tag{6}$$

where the Bowen ratio (β, unitless) is

$$\beta = \gamma\frac{T_a - T_c}{e_a - e_c} \tag{7}$$

where γ is psychrometric constant (kPa K^{-1}), T_a and T_c are the temperature of the air 2 m above and at the canopy layer (°C), respectively, and e_a and e_c are the water vapour pressure (kPa) 2 m above and at the canopy layer, respectively.

2.3 Processing of seasonal data

The data were collected for 183 days during the growing season of 2008. Albedo (ratio of reflected to incoming short-wave solar radiation) and air temperature at 0.3 m were evaluated. The data were divided according to the amount of total incoming short-wave solar irradiance per day into three groups: overcast (0–3000 Wh m^{-2}), cloudy (3000–6000 Wh m^{-2}) and clear (over 6000 Wh m^{-2}). For a detailed description of data processing and seasonal data on incoming, reflected radiation, air temperature and relative air humidity (0.3 m, 2 m) at five different sites, see Huryna and Pokorný (2010).

2.4 Application of satellite data

Satellite data were used to evaluate the relationship between land surface temperature and land cover. Remotely sensed data were obtained by processing Landsat 5 TM scene, which was acquired on 29 July 2008, 9:38 GMT + 1. The satellite data with resolution of 30 m in VIS, NIR and SWIR spectral bands and 120 m in thermal spectral band were

rectified with an S-JTSK coordinate system and resampled by applying the nearest neighbour method to preserve the original radiometric values for subsequent data processing. The data was radiometrically corrected using the Cos(t) model (Chavez, 1996) with calibration coefficients described by Chander et al. (2009). Land surface temperature was computed using the THERMAL Idrisi 15 Andes module (Clark Labs, 2006). To get the real surface temperature, the surface emissivity, (ε), was computed from NDVI using the NDVI Threshold Method ($NDVI^{THM}$) described by Sobrino (2004): for NDVI < 0.2 ε was obtained from red Landsat 5 TM band, for NDVI > 0.5 ε was set 0.99 and for rest of the NDVI scale ($0.2 \leq NDVI \leq 0.5$)ε was computed as follows:

$$\varepsilon = 0.004 P_V + 0.986 \tag{8}$$

where

$$P_V = \left(\frac{NDVI - NDVI_{min}}{NDVI_{max} - NDVI_{min}} \right)^2 \tag{9}$$

where $NDVI_{min} = 0.2$ and $NDVI_{max} = 0.5$.

2.5 Land surface temperatures by thermovision

A thermographic IR FPA camera ThermaCAM^{TM} PM695 (Flir System Sweden) installed on the aircraft Cessna TU 206F was used for temperature mapping of landscape. The aircraft operated by the ArgusGeo s.r.o. company is equipped with gyro-stabilisation and other instruments allowing precise navigation. Pixel size of thermo-images is 2 m. The thermal pictures were done at about 1 pm on 29 July 2008. For more details, see Jirka et al. (2009).

2.6 Conversion of solar energy via transpiration

The transpiration of forest stands was estimated on the basis of sap flow measurements in tree stems, allowing continuous records over long periods under any terrain and environmental conditions. The Trunk Heat Balance (THB) method was applied for oak and the Heat Field Deformation (HFD) method for pine in studies of tree sap flow rates. Stand transpiration was calculated by upscaling the flow data measured in a series of well-selected trees over a range of tree size, using the method of quantiles of total (Čermák et al., 2004).

The THB method is characterised by direct electric heating and internal sensing of temperature and sensors integrating the radial sap flow profile by technical averaging within wide stem sections, applying two to four such sensors per sample tree (Čermák et al., 2004; Tatarinov et al., 2005). The current is automatically distributed in the xylem along the electrodes, reaching the heartwood edge even when the electrodes in the sapwood do not reach it. The THB sensors integrate the radial sap flow profile by technical averaging within the wide stem sections.

The HFD method is based on measurement of the deformation of the heat field around a needle-like linear heater inserted into the stem in a radial direction (Nadezhdina et al., 2006). The HFD method has unique capabilities for measuring the real vector of sap flow rate zero flow as well as reversed flow. A series of multi-point sensors were

used, allowing measurements of radial patterns of sap flow (Čermák and Nadezhdina, 1998; Nadezhdina et al., 2007), so altogether 48 points were used for characterising the conductive system of each sample tree.

3 Results

3.1 Solar energy and temperature in Třeboň ecosystems

The average daily courses of incoming solar radiation were similar at all sites in Třeboň (Figure 2). The average maximum solar radiation fluxes reached about 250 W m^{-2}, 600 W m^{-2} and 890 W m^{-2} on overcast, cloudy and clear days, respectively. The incoming solar radiation on the Wet Meadow was slightly lower than that at other sites on clear days, perhaps due to higher fog formation in the terrain depression of this habitat. The mean daily fluxes ranged from 80.4 W m^{-2} to 83.5 W m^{-2}, from 191.3 W m^{-2} to 293.9 W m^{-2}, and from 286.3 W m^{-2} to 293.9 W m^{-2} on overcast, cloudy and clear days, respectively. The mean daily values of incoming solar energy at five sites on clear days ranged from 7.06 kWh m^{-2} in the field to 6.87 kWh m^{-2} in the Wet Meadow. The amount of reflected short-wave radiation differed markedly between the sites (Figure 3). The reflection of the solar radiation was always lowest at the open water surface, not exceeding 50 W m^{-2}, even on clear days. On clear days, reflection as high as 220 W m^{-2} was measured on the concrete surface. On clear days, the highest mean flux of reflected solar radiation (76.93 W m^{-2}) was at the concrete surface. The fish pond showed the lowest value of mean reflected solar radiation (24.66 W m^{-2}). The mean fluxes of reflected solar energy at the remaining sites were close to each other (about 60 W m^{-2}). The highest daily average of reflected solar radiation on clear days was 1.85 kWh m^{-2} at the concrete surface and the lowest average value of the daily-reflected solar radiation was 0.59 kWh m^{-2} at the fish pond.

Figure 2 The average daily series of the incoming short-wave solar radiation on overcast, cloudy and clear days on five different sites in vegetation season 2008

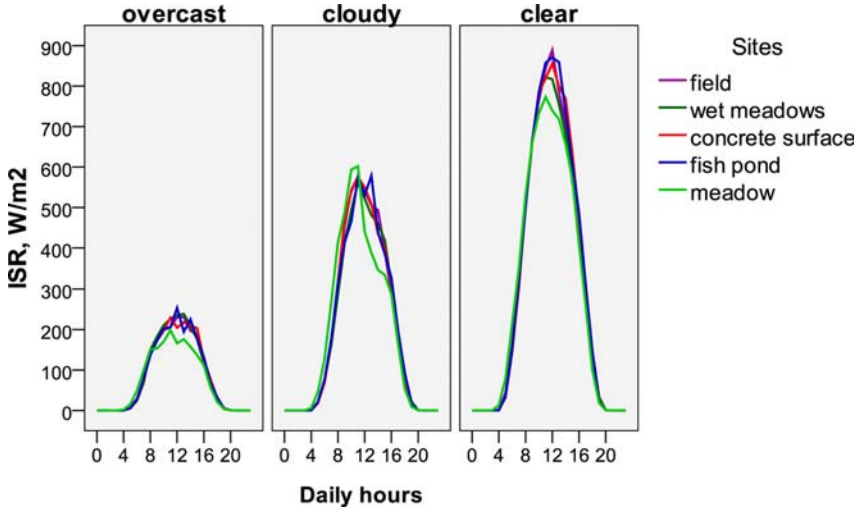

Figure 3 Average daily series of reflected short-wave radiation on overcast, cloudy and clear days on five different sites in vegetation season 2008

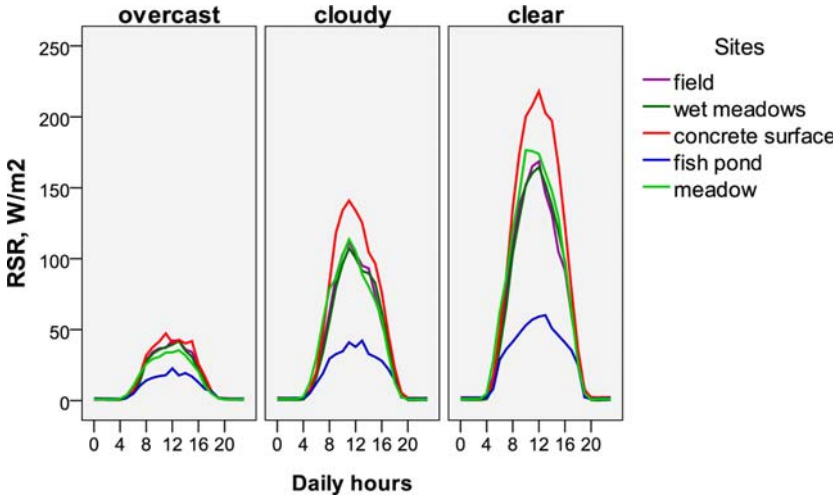

The daily mean time courses of albedo – defined as the ratio of reflected to incoming solar radiation – are shown in Figure 4. The average albedo of the water surface was always the lowest of evaluated sites (about 10%). The albedo of the concrete surface was about 25% on both cloudy and clear days. On overcast days, it was about 20% at this site. Albedo for other sites was about 20% under all irradiance conditions. The high values of albedo in the early morning and late afternoon hours were caused by dividing very small numbers of both variables of the ratio, i.e., incoming and reflected solar radiation, therefore do not provide much useful information.

Figure 4 Average daily series of albedo on overcast, cloudy and clear days on five different sites in vegetation season 2008

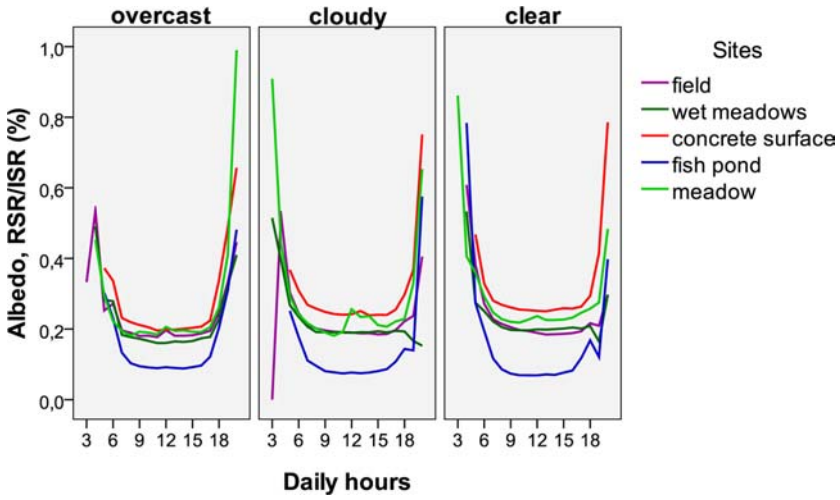

The daily mean courses of the air temperature above ground (30 cm) for overcast, cloudy and clear days are plotted in Figure 5. On clear days at 30 cm, the lowest average midday temperature was at the fish pond; the other sites had similar midday temperatures. On overcast days, the mean temperature was similar at all sites during the whole day. Low early morning temperature in the Wet Meadow can be explained by the terrain depression of the flood area of Rožmberk fish pond. The early morning temperature was on average highest in the fish pond due to the high heat capacity of its water. On overcast days, the difference of mean temperature between the sites ranged from 10.2°C (Wet Meadow) to 11.8°C (fish pond). On cloudy and clear days, the lowest mean temperature was measured at the Wet Meadow (14.08 and 15.58°C, respectively). On clear days, the average difference of temperature between the Wet Meadow and the concrete surface was 3.58°C.

Figure 5 Average daily series of air temperature above ground (30 cm) for overcast, cloudy and clear days on five different sites in vegetation season 2008

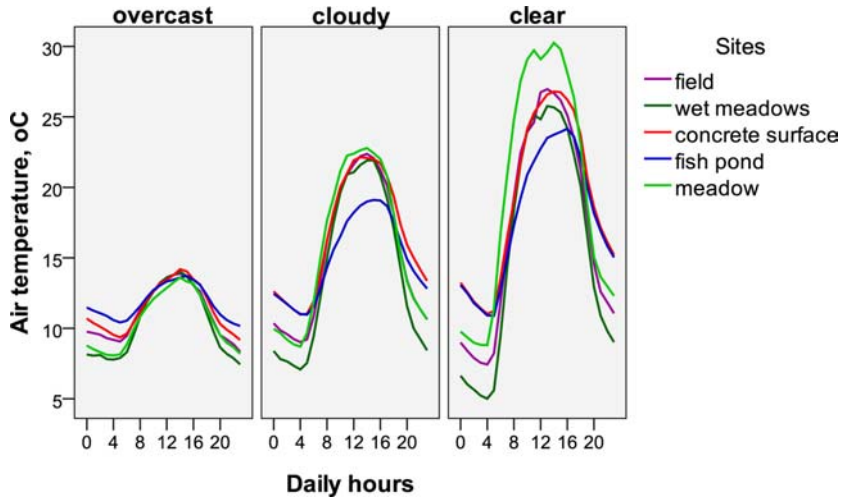

3.2 Energy fluxes at four sites on a sunny day

The daily series of incoming short-wave radiation measured on a sunny day of 29 July 2008 on four sites are plotted in Figure 6(A). The maximum values of incoming radiation are over 800 W m^{-2}. Maximum values on Meadow and Wet Meadow were lower due to local small clouds. Reflected radiation is plotted in Figure 6(B), maximum values range from 150 W m^{-2} (Wet Meadow) to 250 W m^{-2} (concrete). The highest albedo was recorded on concrete, the lowest albedo (less than 20%) was measured on the field and Wet Meadow (Figure 7). Net radiation corrected for IR fluxes is plotted in Figure 8(A). The highest maximum of net radiation was shown by the field and the lowest maximum was estimated for the Meadow. Values of ground heat fluxes differ markedly (Figure 8(B)): the highest ground heat fluxes were shown by concrete and field soil; estimates for the Meadow and the Wet Meadow were lower. Sensible and latent heat fluxes plotted in Figure 8(C) and (D) reach values several hundred W m^{-2}. The highest sensible heat was shown by the concrete and the field. In both Meadows, solar energy

was converted mostly into ET – sensible heat flux was relatively low whereas latent heat fluxes reached a maximum between 400 and 500 W m^{-2}, which corresponds to ET rate up to 0.2 g m^{-2} s^{-1}.

Figure 6 Daily series of incoming short-wave radiation: (A) and outgoing (reflected) short-wave radiation and (B) measured on a sunny day of 29 July 2008 on four sites

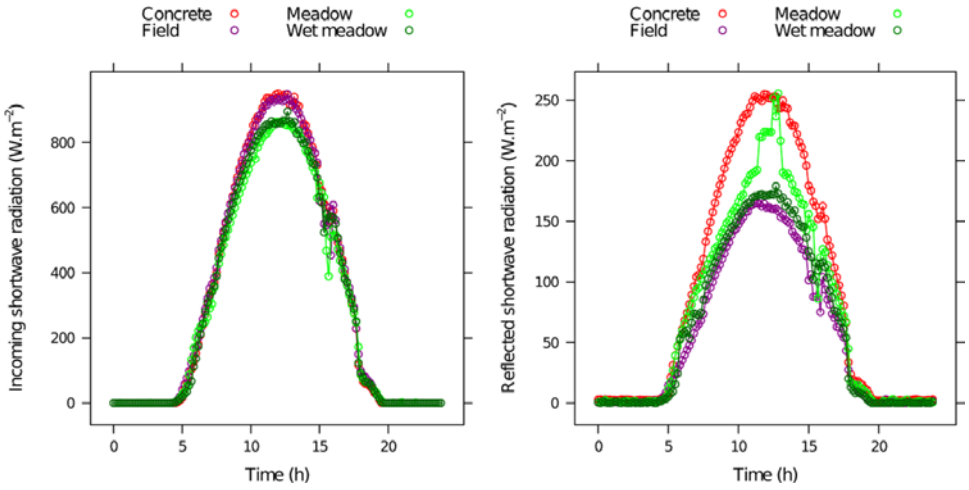

Figure 7 Daily series of albedo of short-wave radiation measured on a sunny day of 29 July 2008 on four sites

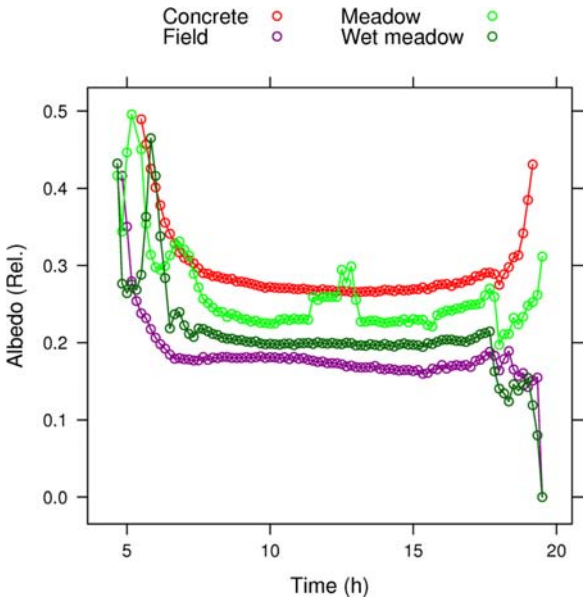

Figure 8 Daily series of energy balance components, total net radiation: (A) ground heat flux; (B) sensible heat flux; (C) latent heat flux and evapotranspiration intensity and (D) on a sunny day of 29 July 2008 on four sites

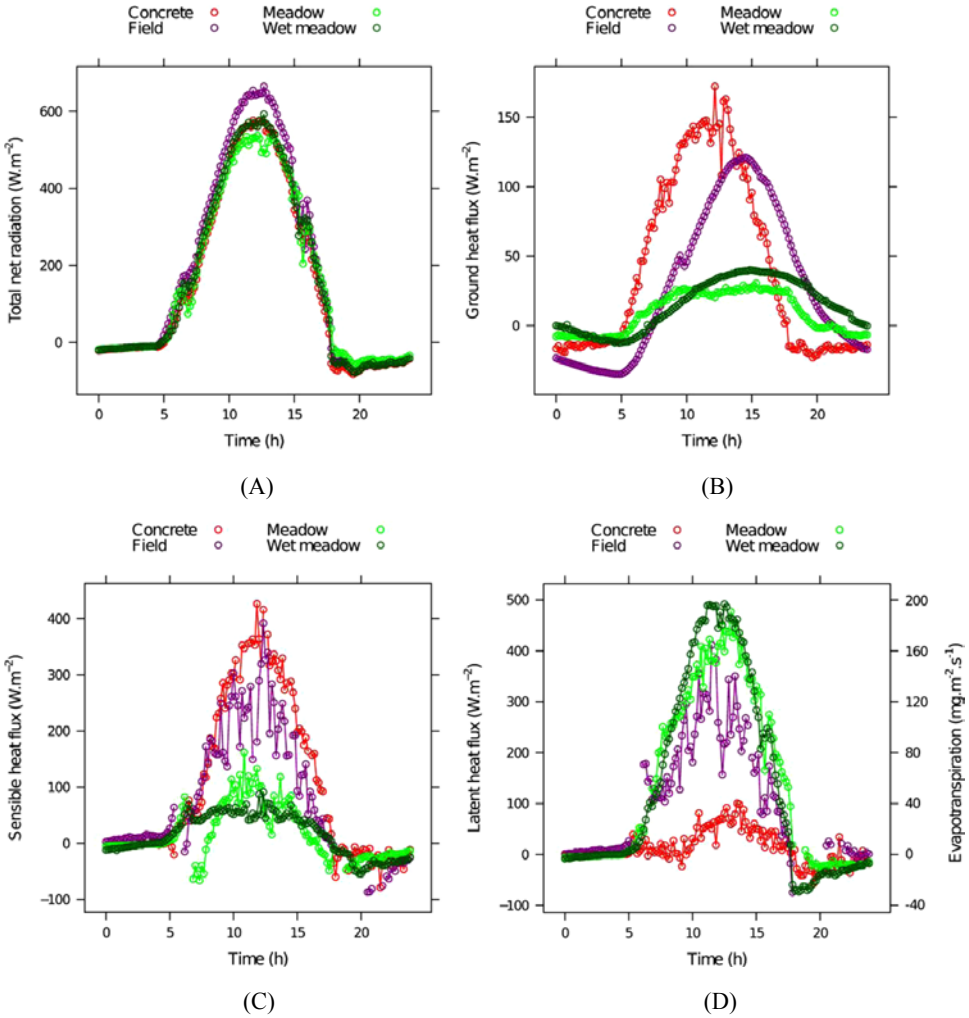

3.3 Satellite images of the Třeboň Landscape

Satellite map of NDVI (Normalised Difference Vegetation Index) highlighting vegetation cover and water bodies and map of surface temperature of the Třeboň Basin are shown in Figure 9. The relatively lower temperature of water bodies and forests (under 20°C) is evident in comparison with higher temperatures of the fields and town of Třeboň (about 25°C). The satellite picture was acquired at 9:38 GMT + 1 as temperature differences between land covers start to develop.

Figure 9 Satellite image of the Třeboň Basin region: (A) a map of vegetation cover using NDVI (Normalised Difference Vegetation Index) and a map of surface temperature and (B) with highlighted water bodies

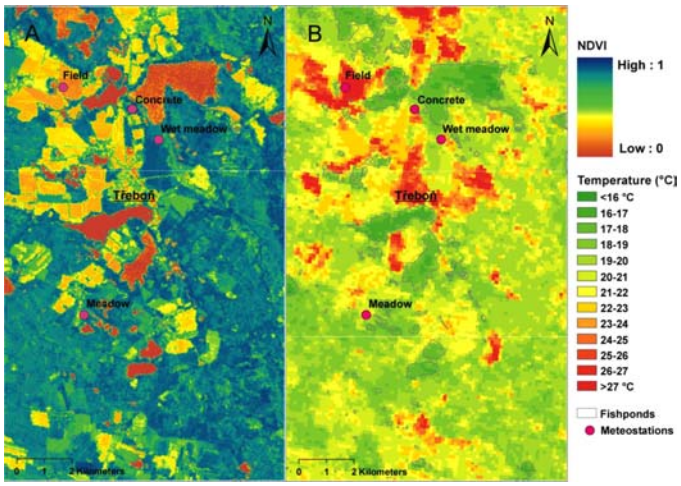

3.4 Detailed map of landscape surface temperature

Surface temperature scanned at about 1 pm GMT + 1 by the thermovision camera around the town Třeboň ranged from 18°C to 42°C, i.e., a 24°C variation (Figure 10). The lowest temperature of around 20°C was shown by water bodies, woods (town park with adult trees) and a large complex of Wet Meadow. The highest temperatures were shown by drained sealed surfaces of the town and mowed Meadow. Drained and harvested fields also showed a very high surface temperature (36–38°C) whereas measures located near water bodies and adult trees gave lower temperatures (about 22°C (Figure 11)).

Figure 10 Surface temperature scanned at c. 1 pm GMT + 1 by the thermovision camera around the town of Třeboň on 29 July 2008

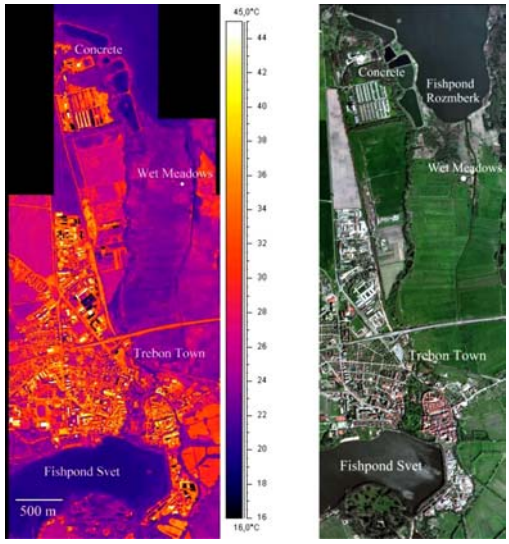

Figure 11 Surface temperature of drained and harvested fields scanned by thermovision camera at c. 1 pm GMT + 1 on 29 July 2008

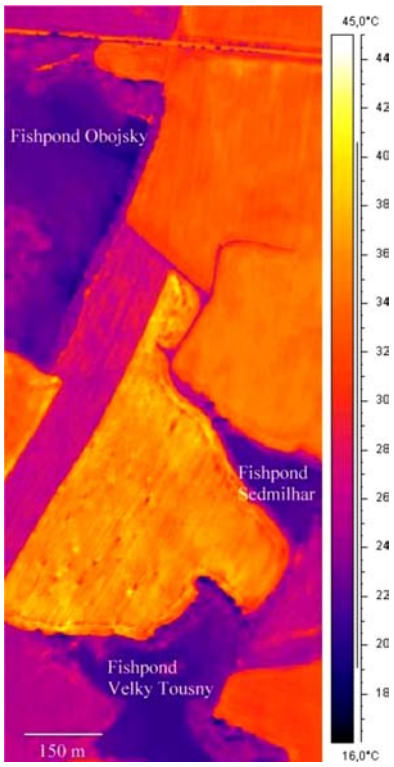

3.5 Conversion of solar energy in forested sites

Direct measurements of dissipated solar energy via transpiration of trees from flood-plain forest and from relatively dry pine forest show marked differences in the amount of transpired water. Flood-plain oaks (*Quercus*) in the growing season transpired about 910 MJ m^{-2} (250 kWh m^{-2}), which corresponds to c. 365 l m^{-2}. Pines in plantation converted via transpiration about 325 MJ m^{-2} (90 kWh m^{-2}), which corresponds to c. 130 l m^{-2} (Figure 13). *Quercus* trees in the flood plain could not transpire much more because of high humidity of the air. The large complex of flood-plain forest in Moravia maintains a humid local climate and therefore PET is about only 40% of incoming radiation. Pine trees are adapted to dry conditions, their needles have several times lower mesophyll cell wall surface than broadleaf species (Nobel, 1991) and the crowns of pines are sparser than that of oaks (Čermák and Prax, 2001; Čermák, 1998; Čermák et al., 2008).

Values for the transpiration of individual oak trees in a flood-plain forest are expressed as MJ m^{-2} per month as shown in Figure 12(A) together with monthly values of potential ET and the amount of incoming solar energy. The amount of solar energy converted into the latent heat of vaporisation of water is about 18% in May and about 30% in June, July, August and September. A proportional relationship between incoming solar radiation and transpiration was evident – trees well supplied with water increased their conversion of radiation according to the amount of incident solar energy and air

humidity (PET). The total amount of solar energy converted during the growing season by means of the latent heat of vaporisation of water (measured as rate of transpiration) is about 910 MJ m^{-2} (250 kWh m^{-2}), which corresponds to about 365 l m^{-2} (Figure 13).

Figure 12 Transpiration of oak (*Quercus*) trees (A) and pines (B) potential evapotranspiration of flood-plain forest (A) and pine plantation (B) and incoming solar radiation to flood-plain forest (A) and pine forest (B) expressed as MJ m^{-2} per month

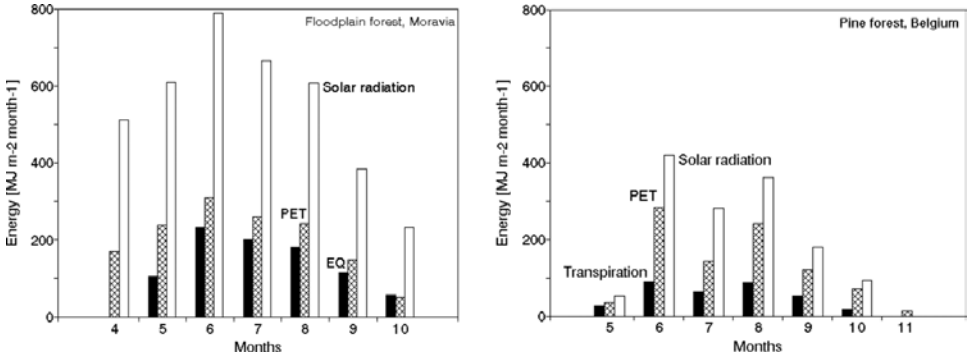

(A) (B)

Figure 13 Amount of solar energy converted via transpiration of pine plantation (Belgium) and oak (*Quercus*) flood-plain forest (Moravia), potential evapotranspiration and income of solar energy to the both sites (MJ m^{-2})

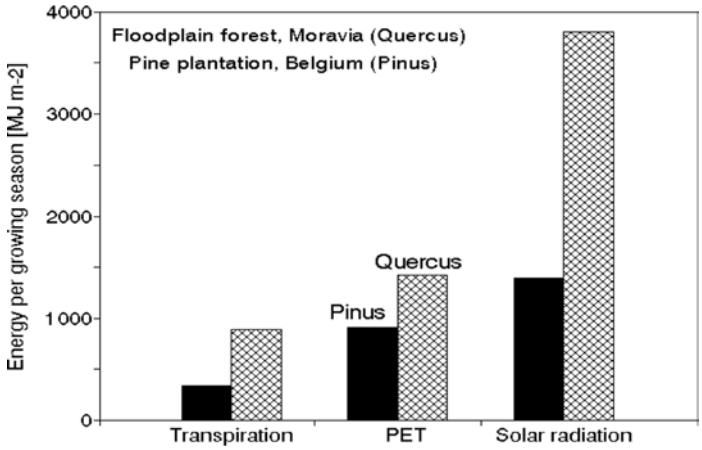

The sap flow method for assessment of transpiration measures the flow of water in a tree trunk. It does not measure the so-called micro-watercycle – evaporation of water from leaves and consequent condensation of water vapour in the night. This water can also be considered as intercepted. However, recent studies show that a certain amount of water can be absorbed by forest canopies and transported via stems, measured as a reverse flow down to roots. This amount of water is much smaller than transpiration, but it is very important under severe drought, and even after short rains, because it allows roots to survive and absorb water as soon as soil water supply is renewed (Nadezhdina et al., 2006).

The transpiration values of individual pine trees in the plantation were expressed as MJ m^{-2} per month as shown in Figure 12(B). The amount of solar energy converted in latent heat of vaporisation of water (measured as transpiration) was about 23%. A relatively higher difference between transpiration and PET indicates either a shortage of water or low ability of the pine to transpire water. The amount of water transpired by *Pinus* during the growing season is equal to 130 l m^{-2} corresponding to the latent heat of vaporisation of water about 325 MJ m^{-2} (90 kWh m^{-2}), see Figure 13.

Transpiration as a fraction of the potential ET for pine and oak is shown in Figure 14. In summer months, there was an evident difference between *Pinus* and *Quercus* – the transpiration from trees in the flood-plain forest is about 90% of PET, i.e., *Quercus* trees are usually not limited by shortage of water there. In the pine plantation, the transpiration of pine trees did not exceed 55% of PET. Potential ET of *Quercus* and Pinus as a fraction of incoming solar radiation are plotted in Figure 15. A remarkably similar PET fraction for *Quercus* from May to September (about 45%) indicates that flood-plain forest maintains or controls the humidity of the air by transpiration from trees.

Figure 14 Transpiration of pine and oak (*Quercus*) as a fraction of potential evapotranspiration for individual months of vegetation season (April–October)

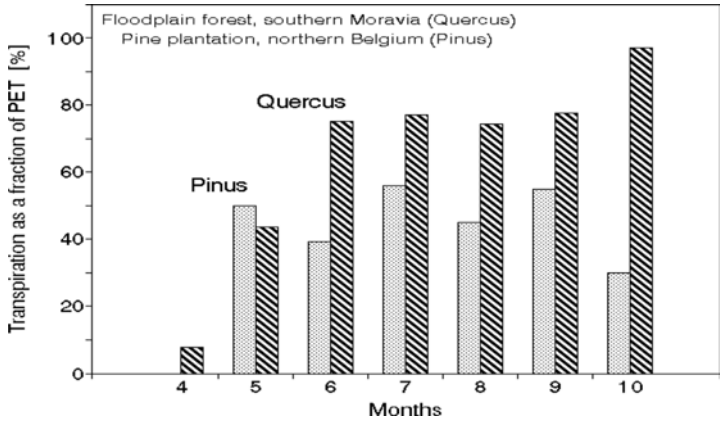

Figure 15 Potential evapotranspiration as a fraction of seasonal income of solar radiation for the flood-plain forest and pine plantation

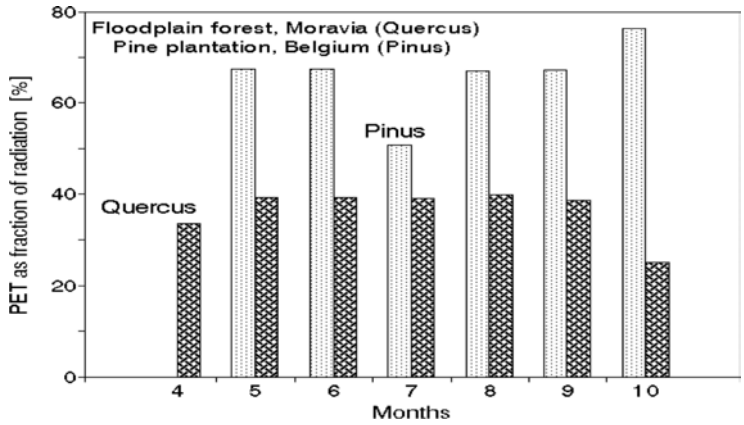

4 Discussion

The surface temperature of a landscape results from the interplay of albedo and distribution of net radiation into the latent heat flux, sensible heat flux, ground heat flux and energy storage in the ecosystem. Surface temperatures on different land covers were found to be similar on overcast days when most of the solar radiation is absorbed and reflected by clouds and there is less than 3 kWh incident on square metre of land surface per day. On cloudy days when incoming radiation ranged between 3 and 6 kWh m^{-2} day^{-1}, the daily series of temperatures differed at early morning and midday: the lowest daily temperature amplitude was shown by fish-pond water. Differences among sites in midday maxima reached 4°C. On clear days when incident solar radiation exceeded 6 kWh m^{-2} day^{-1}, mean temperature differences among sites reached c. 7°C at both early morning and midday. The lowest daily amplitude, highest early in the morning and lowest at midday values, was shown at the fish pond. The high midday temperature of the Meadow can be caused by the mulch, which insulates soil and reduces ground heat flux. The average temperature calculated from data measured for the whole growing season was high at the concrete surface both at 30 cm (16.09°C) and 2 m (15.73°C).

The concrete surface was the site of highest albedo (25%), but it was not albedo that decreased temperature. Low temperature was measured at the Wet Meadow and other vegetated sites. The fish pond, which was the site of lowest albedo c. 10% (see Figures 3 and 4), had the lowest temperature reading 0.3 m above water level (Figure 5). Dense concrete has a relatively high thermal conductivity (1.5 W m^{-1} K^{-1}) and high heat capacity: 2.11 J m^{-3} $K^{-1} \times 10^6$ (Oke, 1987). The heat capacity of water is twice as high as dense concrete (4.18 J m^{-3} $K^{-1} \times 10^6$). Despite a high albedo, the concrete surface had highest temperature maxima and highest daily temperature amplitude. The latent heat of vaporisation of water is three orders of magnitude higher than the heat capacity of dense concrete (2.5 J m^{-3} $K^{-1} \times 10^9$). Thus, surfaces are cooled during vaporisation and warmed during condensation of water. Water bodies and forests have the lowest surface temperature in a landscape on a sunny day (both thermovision and satellite thermal pictures confirm this (Figures 9–11)).

Some scientific papers argue that the low albedo of forests contributes to global warming (Gibbard et al., 2005). For example, Randerson et al. (2006) conclude that "future increases in boreal fire may not accelerate climate warming". Bala et al. (2007) claim that

> "global-scale deforestation has a net cooling influence on climate, because the warming carbon-cycle effects of deforestation are overwhelmed by the net cooling associated with changes of albedo and ET."

However, the cooling effect of forests on hot sunny days is confirmed by Figures 9–11. Likewise, thermal satellite pictures from Hesslerová and Pokorný (2010a, 2010b) show the low surface temperature of forested areas. The data strongly suggest that it is not albedo that controls the damping of temperature with high incoming solar radiation. It is the interaction of water and plants that dampens temperature maxima.

The detailed study of solar energy distribution on a summer sunny day in the four Třeboň sites has shown that the most vigorous fluxes are linked with sensible heat or with the latent heat of ET. In dry places, the sensible heat flux reached values over 300 W m^{-2} whereas vegetation well supplied with water will convert over 400 W m^{-2} into cooling ET. The daily curve of latent heat or ET shows a feedback

coupling between incoming solar radiation and the rate of ET – ET increases with incoming solar energy reaching its maximum at about midday. These effects both concur with everyday experience, and are described quantitatively by Budyko (1974), Monteith and Unsworth (1990) and Bonan (2008) among others. However, findings on the principal role of water and plants in the distribution of solar energy and temperature control of ecosystems are not emphasised in policy recommendations issued by the Intergovernmental Panel on Climate Change (IPCC, 2007).

In the present investigation, temperature maps of the landscape taken both by satellite images and by airborne thermo-camera clearly evidence temperature differences between land covers. On a sunny day, the highest temperatures were in sealed urban areas and on harvested drained fields. At about midday, the difference between vegetated areas and sealed surfaces reached 14°C over an area of several square kilometre in the flat Třeboň Basin region. The satellite image taken, the same day at 9:30, showed smaller temperature differences with forests, wet Meadow and water bodies being the coolest sites. Satellite pictures taken in Northwest Bohemia at the same time showed temperature differences of almost 20°C between large drained areas such as open cast mines and fields vs. forests (Hesslerová and Pokorný, 2010a). Likewise, the deforestation of large areas in tropical regions may result in a temperature increase of about 20°C (Hesslerová and Pokorný, 2010b). The consequent turbulent flow of hot air of low relative humidity affects the surrounding ecosystems and may contribute to the melting of mountain glaciers.

Differential heating caused by sensible heat gradients across adjacent regions of intensively transpiring vegetation and dry, bare, soil can generate a sea breeze-like circulation, called 'vegetation breeze' (Eltahir and Bras, 1996; Pielke, 2001, 2005; McPherson, 2007). Lawton et al. (2001) have shown that land-use change in tropical lowlands has serious impacts on ecosystems in adjacent mountains. Landsat and Geostationary Operational Environmental Satellite imagery shows deforested parts of Costa Rica's Caribbean lowlands remain relatively cloud-free, whereas forested regions develop dry season cumulus cloud fields. These conditions facilitate maintenance of the short water circuit essential to re-coupling the water and carbon cycles (Ripl, 2003).

Land drainage for agriculture or urbanisation usually means a loss of vegetation, resulting in a shift from the self-regulating dissipative structures described earlier, to negative consequences such as temperature swings leading to turbulent motion in warm dry air. In relation to global warming, it is recognised that while humans induce CO_2 emissions by land clearing and burning fossil fuels, ecosystems bind CO_2 in the biomass of plants and soil. What is less often realised is the fact that the annual increase in humanly induced carbon in the atmosphere is an amount equivalent to only 0.6% of the carbon contained in vegetation and 0.2% of the carbon contained in soils. Studies by Beran (1994) and IPCC (2007) put the annual increment of carbon in the atmosphere from CO_2 emissions at 3.5 GT. In soil, there is c. 2000 GT of naturally occurring carbon; in vegetation 610 GT and in the atmosphere 750 GT of carbon. These various sources exchange carbon in a functional relation to each other, a dynamic that is uncoupled when local water cycles are damaged. This lost functioning is observed on a global scale in the Millennium Environmental Assessment (2005), which notes that every year, some 60,000 km^2 of badly managed land is becoming desert. About 200,000 km^2 of land loses agricultural productivity as people in development projects or farmers themselves cut down plants and drain soils. The drying out and loss of ecosystem function now affects 30–40% of the global landmass.

When carbon is fixed in biomass via photosynthesis, this consumes a relatively small amount of solar energy. However, photosynthesis is accompanied by transpiration of water, which transfers solar energy at two orders of magnitude higher than photosynthesis. The restoration of water and plants to arid areas can sequester substantial amounts of emitted carbon, as well as simultaneously improve land productivity and temperature extremes. The largest data collection on the regenerative capacity of global ecosystems is the International Biological Programme (Cooper, 1975), which estimates that plants produce annually 1 kg dry biomass per m^2 in temperate zones and up to 5 kg m^2 in the tropics. Now, 1 kg of dry biomass contains 0.4 kg of carbon. Thus, to sequester an annual increment of 3.5 GT of carbon (IPCC, 2007), each m^2 of land would need to bind an additional amount of 0.02 kg of carbon. This could be achieved if the 40% of global landmass that currently lacks water and vegetation capacity were restored, because plant binding of an additional 58 metric tons of carbon per km^2 year (0.058 kg m^{-2}) can compensate for 3.5 GT. Given wide public concern about CO_2 levels, it makes sense to enhance ecological functioning to its maximum capacity.

The control of human impacts on landscapes is desirable for a number of reasons and this study clarifies one of these – the self-regulatory damping of solar radiation in a healthy ecosystem. Plant stands supplied with water are able to respond to incoming solar energy to an order of magnitude of hundreds W m^{-2}. This dissipative structure receives energy pulses from outside and reacts with a positive feedback loop, which is unlike the classic amplifying feedback regarded as destructive in cybernetics. The responses of an ecosystem to incoming solar energy function as a source of new order and complexity (Capra, 1996). Currently, the IPCC (2007) does not engage adequately with the complex interplay of water, sunlight and vegetation. It tends to focus on correlations between artificially generated average Earth temperatures, on the one hand, and concentrations of specific greenhouse gases, on the other. Levels of atmospheric CO_2 increased during the past 250 years from c. 280 ppm to 360 ppm. The IPCC documents the radiative forcing caused by an increase in greenhouse gases in the atmosphere from 1750 is equal to 1–3 W m^{-2}. In the next 10 years, the radiative forcing is expected to increase by 0.2 W m^{-2}. Comparing these values with the amount of water in the atmosphere, the ability of ecosystems to distribute solar energy, and the value and time variability of the solar constant (1345–1438 W m^{-2} during one year), it is difficult to understand why the IPCC does not give more attention to the climatic effects of ecosystem processes.

5 Conclusion

Functioning ecosystems cool themselves; they use solar energy for self-organisation and export entropy to the atmosphere as heat. These energy transformations are achieved by water and plants in the activity of ET. In this study, the dissipative process is demonstrated by data collected at seven sites in the Czech Republic and Belgium, with analysis of landscape temperatures assisted by thermovision and satellite images. Implications of the research for understanding climate change are discussed.

Acknowledgement

The study was supported by the grants of MSMT Czech Republic NPV 2B06023 and VZ MSM 6215648902.

References

Bala, G., Caldeira, K., Wickett, M., Phillips, T.J., Lobell, D.B., Delire, C. and Mirin, A. (2007) 'Combined climate and carbon cycle effects of large-scale deforestation', *PNAS*, Vol. 104, No. 16, pp.6550–6555.

Beran, M.A. (1994) *Carbon Sequestration in the Biosphere: Process and Prospects*, NATO ASI Series, Springer, New York.

Berry, S.L., Farquhar, G.D. and Roderick, M.L. (2005) 'Co-evolution of climate, vegetation, soil and air', in Blöschl, G. and Sivapalan, M. (Eds.): *Encyclopedia of Hydrological Sciences*, Vol. 1, Wiley, Chichester, UK.

Bonan, G. (2008) *Ecological Climatology*, Cambridge University Press, New York.

Brutsaert, W. (1982) *Evapotranspiration into the Atmosphere: Theory, History and Applications*, Reidel, Dordrecht.

Budyko, M.I. (1974) *Climate and Life*, Academic Press, New York.

Capra, F. (1996) *The Web of Life: A New Synthesis of Mind and Matter*, Harper, New York.

Chander, G., Markham, B.L. and Helder, D.L. (2009) 'Summary of current radiometric calibration coefficients for Landsat MSS, TM, ETM+, and EO-1 ALI sensors', *Remote Sensing of Environment*, Vol. 113, No. 5, pp.893–903.

Chavez, P.S. (1996) 'Image-based atmospheric corrections: revisited and improved', *Photogrammetric Engineering and Remote Sensing*, Vol. 62, No. 9, pp.1025–1036.

Clark Labs (2006) IDRISI 15 The Andes Edition. Clark University, Worcester, MA.

Cooper, J.P. (1975) *Photosynthesis and Productivity in Different Environments*, Cambridge University Press, London.

Čermák, J. and Nadezhdina, N. (1998) 'Sapwood as the scaling parameter – Defining according to xylem water content or radial pattern of sap flow?', *Ann. Sci. For.*, Vol. 55, pp.509–521.

Čermák, J. (1998) 'Leaf distribution in large trees and stands of the floodplain forests in southern Moravia', *Tree Physiol.*, Vol. 18, pp.727–737.

Čermák, J., Riguzzi, F. and Ceulemns, R. (1998) 'Scaling up from the individual trees to the stand level in Scots pine: 1. Needle distribution, overall crown and root geometry', *Ann. Sci. For.*, Vol. 55, pp.63–88.

Čermák, J. and Prax, A. (2001) 'Water balance of the floodplain forests in southern Moravia considering rooted and root-free compartments under contrasting water supply and its ecological consequences', *Ann. Sci. For.*, Vol. 58, pp.1–12.

Čermák, J., Kučera, J. and Nadezhdina, N. (2004) 'Sap flow measurements with two thermodynamic methods, flow integration within trees and scaling up from sample trees to entire forest stands', *Trees, Structure and Function*, Vol. 18, pp.529–546.

Čermák, J., Nadezhdina, N., Meiresonne, L. and Ceulemans, R. (2008) 'Scots pine root distribution derived from radial sap flow patterns in stems of large leaning trees', *Plant and Soil*, Vol. 305, Nos. 1–2, pp.61–75.

Eltahir, E.A.B. and Bras, R.L. (1996) 'Precipitation recycling', *Reviews of Geophysics*, Vol. 34, No. 3, pp.367–378.

Gates, D.M. (1980) *Biophysical Ecology*, INC, Dover.

Geiger, R., Aron, R.H. and Todhunter, P. (2003) *The Climate Near the Ground*, Rowman & Littlefield, Lanham, ML.

Gibbard, S., Caldiera, K., Bala, G., Philips, T.J. and Wickett, M. (2005) 'Climate effects of global land cover change', *Geophysical Research Letters*, Vol. 32, p.L23705.

Hesslerová, P. and Pokorný, J. (2010a) 'The synergy of solar radiation, plant biomass, and humidity as an indicator of ecological functions of the landscape: a case study from Central Europe', *Integrated Environmental Assessment and Management*, Vol. 6, No. 2, pp.249–259.

Hesslerová, P. and Pokorny, J. (2010b) 'Forest clearing, water loss, and land surface heating as development costs', *International Journal of Water*, Vol. 5, No. 4, pp.401–418.

Huryna, H. and Pokorný, J. (2010) 'Comparison of reflected solar radiation, air temperature and relative air humidity in different ecosystems', in Vymazal, J. (Ed.): *Water and Nutrient Management in Natural and Constructed Wetlands*, Springer, New York, pp.309–326.

IPCC (2007) *Climate Change – Synthesis Report*, in Pachauri, R.K. and Reisinger, A. (Eds.), http://www.ipcc.ch/ (accessed 16 February 2010).

Jassal, J.R., Black, A.T., Cai, T., Morgenstern, K., Li, Z., Gaumont-Guay, D. and Nesic, Z. (2007) 'Components of ecosystem respiration and an estimate of net primary productivity of an intermediate-aged Douglas-fir stand', *Agricultural and Forest Meteorology*, Vol. 144, pp.44–57.

Jeník, J. and Květ, J. (2002) 'Human impacts on the Třeboň basin biosphere reserve', in Květ, J., Jeník, J. and Soukupová, L. (Eds.): *Freshwater Wetlands and their Sustainable Future: A Case study of Třeboň Basin Biosphere Reserve*, UNESCO Man and the Biosphere Series, Czech Republic, Paris, Vol. 28, pp.3–10.

Jirka, V., Hofreiter, M., Pokorný, J. and Novák, M. (2009) 'Method for Estimation of surface fluxes of Solar energy in landscape based on Remote sensing', Paper presented at the *6th International Conference on Environmental Hydrology*, September, Cairo, F – Irrigation, pp.1–13.

Jones, H.G. (1992) *Plants and Microclimate: A Quantitative Approach to Environmental Plant Physiology*, Cambridge University Press, London.

Kopp, G., Lawrence, G. and Rottman (2005) 'The total irradiance monitor (TIM): science results', *Solar Physics*, Vol. 230, No. 1, pp.19–140.

Kučerová, A., Pokorný J., Radoux, M., Němcová, M., Cadelli, D. and Dušek, J. (2001) 'Evapotranspiration of small-scale constructed wetlands planted with ligneous species', in Vymazal, J. (Ed.): *Transformations of Nutrients in Natural and Constructed Wetlands*, Backhuys, Leiden.

Lambers, H., Chapin, F.S. and Pons, T.L. (1998) *Plant Physiological Ecology*, Springer, New York.

Lawton, R.O., Nair, U.S., Pielke Sr., R.A. and Welch, R.M. (2001) 'Climatic impact of tropical lowland deforestation on nearby Montana cloud forests', *Science*, Vol. 294, No. 5542, pp.584–587.

Li, L. and Yu, Q. (2007) 'Quantifying the effects of advection on canopy energy budgets and water use efficiency in an irrigated wheat field in the North China Plain', *Agricultural Water Management*, Vol. 89, Nos. 1–2, pp.116–122.

McPherson, R.A. (2007) 'A review of vegetation-atmosphere interactions and their influences on mesoscale phenomena', *Progress in Physical Geography*, Vol. 31, No. 3, pp.261–28.

Millennium Environmental Assessment (MEA) (2005) *Ecosystems and Human Well-being: Desertification Synthesis*, World Resources Institute, Washington DC.

Monteith, J.L. (1975) *Vegetation and Atmosphere*, Academic Press, London.

Monteith, J.L. and Unsworth, M. (1990) *Principles of Environmental Physics*, Butterworth, Oxford.

Nadezhdina, N., Čermák, J., Gašpárek, J., Nadezhdin, V. and Prax, A. (2006) 'Vertical and horizontal water redistribution inside Norway spruce (Picea abies) roots in the Moravian upland', *Tree Physiology*, Vol. 26, pp.1277–1288.

Nadezhdina, N., Čermák, J., Meiresonne, L. and Ceulemans, R. (2007) 'Transpiration of Scots pine in Flanders growing on soil with irregular substratum', *Forest Ecology and Management*, Vol. 243, No. 1, pp.1–9.

National Oceanic and Atmospheric Administration (NOAA) (2010) *State of the Climate Global Analysis*, NCDC National Climatic Data Center, July, Asheville, NC.

Nobel, P.S. (1991) *Physicochemical and Environmental Plant Physiology*, Harcourt Brace, New York.

Oke, T.R. (1987) *Boundary Layer Climates*, Methuen, London.

Peters-Lidard, C.D., Blackburn, E., Liang, X. and Wood, E.F. (1998) 'The effect of soil thermal conductivity parameterisation on surface energy fluxes and temperatures', *Journal of the Atmospheric Science*, Vol. 55, pp.1209–1224.

Pielke Sr., R.A. (2001) 'Influence of the spatial distribution of vegetation and soils on the prediction of cumulus convective rainfall', *Reviews of Geophysics*, Vol. 39. No. 2, pp.151–177.

Pielke Sr., R.A. (2005) 'Land use and climate change', *Science*, Vol. 5754, No. 310, pp.1625–1626.

Randerson, J.T., Liu, H., Flanner, M.G., Chambers, S.D., Jin, Y., Hess, P.G., Pfister, G., Mack, M.C., Treseder, K.K., Welp, L.R., Chapin, F.S., Harden, J.W., Goulden, M.L., Lyons, E., Neff, J.C., Schuur, E.A. and Zender, C.S. (2006) 'The impact of boreal forest fire on climate warming', *Science*, No. 314, pp.1130–1132.

Ripl, W. (1995) 'Management of water cycle and energy flow for ecosystem control: the energy-temperature-reaction (ETR) model', *Ecological Modelling*, Vol. 78, Nos. 1–2, pp.61–76.

Ripl, W. (2003) 'Water: The bloodstream of the biosphere', *Philosophical, Transactions of the Royal Society of London*, Vol. B358, No. 1440, pp.1921–1934.

Schneider, E.D. and Sagan, D. (2005) *Into the Cool: Energy Flow, Thermodynamics, and Life*, University of Chicago Press, Chicago.

Sobrino, J. (2004) 'Land surface temperature retrieval from LANDSAT TM 5', *Remote Sensing of Environment*, Vol. 90, Nos. 3–4, pp.434–440.

Tatarinov, F.A., Kučera, J. and Cienciala, E. (2005) 'The analysis of physical background of tree sap flow measurements based on thermal methods', *Measuring Sci. and Technol.*, Vol. 16, pp.1157–1169.

Vasicek, F. (1985) 'The shrub layer in the ecosystem of the floodplain forest', in Penka, M., Vyskot, M., Klimo, E. and Vasicek, F. (Eds.): *Floodplain Forest Ecosystem I: Before Water Management Measures*, Elsevier, Amsterdam.

You, Ch.Y., Pence, H.E., Hasegava, P.M. and Mickelbart, M.V. (2009) 'Regulation of transpiration to improve crop water use', *Critical Reviews in Plant Sciences*, Vol. 28, No. 6, pp.410–431.